J. Marine Env. Engg., Vol. 5, pp. 311–349
Reprints available directly from the publisher
Photocopying permitted by license only

THE IMPACT OF A HIGH DISCHARGE EVENT ON THE STRUCTURE AND EVOLUTION OF THE CHESAPEAKE BAY PLUME BASED ON MODEL RESULTS*

L. C. BREAKER[a,†], J. G. W. KELLEY[a,‡], L. D. BURROUGHS[a], J. L. MILLER[b], B. BALASUBRAMANIYAN[c] and J. B. ZAITZEFF[d,¶]

[a] *National Centers For Environmental Prediction, Camp Springs, Maryland 20746-4304;* [b] *Naval Research Laboratory, Stennis Space Center, MS 39529;* [c] *General Sciences Corporation, Laurel, MD 20707;* [d] *National Environmental Satellite Data and Information Service, Camp Springs, Maryland 20746-4304*

(Received May 1999; In final form August 1999)

A study was conducted to determine how well a quasi-operational ocean forecast model, given its present configuration and constraints, could reproduce and characterize a mesoscale circulation feature near the U.S. East Coast, specifically the Chesapeake Bay plume. A secondary goal was to determine the impact of anomalous discharge from the Bay on the circulation over the adjacent shelf, following a major precipitation event, Hurricane Fran. Two model runs were conducted for the period from mid-August through mid-September, 1996. One run used a discharge function based on daily "observed" river inflows to the Bay. The second run employed the climatological data used routinely in the model. Both runs employed realistic tidal forcing and surface winds from a high-resolution atmospheric forecast model.

The primary outflow following Hurricane Fran, based on the observed discharge function, was concentrated over a period of just a few days, producing what was expected to be the maximum impact on the behavior of the plume. For comparison, observations of surface salinity acquired from a recently-developed airborne microwave

* OMB Contribution No. 157.

† Corresponding author.

‡ John Kelley was a UCAR visiting postdoctoral scientist at NCEP when this work was begun. He now works for the National Ocean Service Coast Survey Development Laboratory in Silver Spring, Maryland.

¶ Deceased.

radiometer are compared with model output fields in the near-field region of the plume ($\leq \sim 20$ km from the mouth of the Bay). Salinity maps from the airborne radiometer showed that the discharge function based on daily stream flow data produced significant improvements in characterizing the near-field region of the plume compared to the monthly climatological outflow time history. The remote observations also revealed a significant reduction in surface salinity near the mouth of the Bay between the 14th and the 19th of September 1996, which was not apparent in the model-generated salinity maps for the same period. This discrepancy is attributed to the inherent difficulties in specifying the initial conditions at the mouth of the Bay.

Although direct verification of the model results could not be made beyond the coverage provided by the airborne radiometer, the model-generated plume exhibited structure and temporal behavior which are consistent with past observations. A separate calculation of the Kelvin number from model output indicated that earth rotation should be important in determining the orientation of the plume. The surface circulation in the far-field region of the plume was strongly influenced by local winds and, to a lesser, extent by the salinity gradients associated with the plume, according to the model results. Also, the structure of the plume responded quickly to rapid changes in outflow from the Bay, to wind forcing, or to both, on time scales of several days or less. A sequence of model-generated salinity profiles along a line close to the axis of the plume indicated that the strength of the halocline weakened, and that the depth of the halocline decreased from roughly 10 m near the mouth of the Bay to 5 m or so at distances of 60–75 km offshore.

Keywords: Chesapeake Bay; plume; coastal ocean forecast system; discharge function; Hurricane Fran; salinity; surface currents; salinity mapper; Kelvin number

1. INTRODUCTION

1.1. General

An ocean forecast system which includes a three-dimensional ocean circulation model, together with a coupled atmospheric forecast model and ocean data assimilation, is nearing completion as the first fully-operational, real-time coastal ocean forecast system to be developed for U.S. coastal waters (*e.g.*, Kelly *et al.*, 1997). This model, called the Coastal Ocean Forecast System (COFS), has been used to make experimental forecasts of the state of the coastal ocean for a region off the U.S. East Coast on a daily basis since 1993. The model domain extends from 27° to 48°N, and from the East Coast out to 50°W, covering an area of roughly 4×10^6 km^2. The model domain was chosen to include the Gulf Stream because of its importance in influencing the circulation closer to the coast. Because of computational considerations, the model's horizontal resolution was selected to be approximately 10 km near the coast. Further offshore the resolution decreases slightly. In the vertical, 18 layers were considered sufficient

to resolve the vertical structure. Given these system parameters, it was the primary goal of this study to determine just how well COFS could reproduce and resolve the important mesoscale structures that are typically found in the coastal ocean such as eddies, jets, fronts, and river plumes? As a case in point, we picked the Chesapeake Bay (CB) plume, a permanent feature located off the mouth of the CB, as the basis for this study.

A number of studies have indicated that winds, tides, and river discharge are three of the most important factors that influence the shelf circulation off the mouth of CB (*e.g.*, Valle-Levinson *et al.*, 1997; Chao, 1988b). In COFS, realistic wind forcing is provided through direct, one-way coupling with a high-resolution atmospheric forecast model. Tidal forcing from the astronomical tides is included in the model for the six primary tidal constituents.[1] Discharge from CB is presently based on the monthly climatology of Blumberg and Grehl (1987). Clearly, the outflow from CB, as specified in the model, is not necessarily realistic since the time scales of variability in outflow can be as short as several days or less. This is especially true for major precipitation events such as tropical storms and hurricanes (*e.g.*, Corps of Engineers, 1975). Consequently, we also examined the response of the model-generated plume to a major perturbation in outflow from the Bay which was reconstructed from river streamflow data following the passage of Hurricane Fran.

Hurricane Fran (HF) made landfall near Cape Fear, North Carolina on September 5, 1996 and deposited 160 to 330 mm (5–10 in) of rain over the middle-Atlantic region with up to 525 mm (16 in) of rain in parts of Virginia and West Virginia (U.S. Department of Commerce, 1997). Much of this precipitation found its way through the CB watershed and into the Bay itself. Over a period of days to several months, this excess fresh water was discharged from the mouth of CB onto the continental shelf. Two aircraft flights were conducted within a two-week period following HF as part of the Naval Research Laboratory's Chesapeake Outflow Plume Experiment (COPE-I; Miller *et al.*, 1998) to infer the surface salinity in a limited region just beyond

[1]Comparisons of model-generated tides with observed tides at various tide gauges along the U.S. East Coast have shown generally good agreement (*e.g.*, Aikman *et al.*, 1998).

the mouth of CB by using a recently-developed Scanning Low-Frequency Microwave Radiometer[2] (Goodberlet *et al.*, 1997).

Model plumes were generated first with monthly climatological outflows and then with the daily "observed" outflows. The daily outflows were estimated by combining stream flow data from the nine largest rivers that feed into CB assuming no significant lags in following the waters from HF through the bay system. The details concerning this assumption are discussed in Section 6. Consequently, our results most likely correspond to the maximum impact that could have occurred on the shelf with respect to the outflow from CB following HF. As a result, we created a stringent test of the model's response to discharge from the Bay. In the model simulations, we considered three cases. The first case corresponds to the time of maximum daily outflow from CB following HF, but included no observed salinity data; the other two cases correspond to times when observed salinities were available. In all cases, salinity, surface and subsurface, and surface currents from the model were used to depict the plume and its evolution.

The text is divided into seven sections which include the introduction (Section 1), a description of the ocean model (Section 2), a brief description of the salinity mapper that was used to produce the salinity maps on the 14th and the 20th of September 1996 (Section 3), an explanation of the model runs and data acquisition procedures (Section 4), the results (Section 5), a discussion of selected topics (Section 6), and a summary and conclusions (Section 7).

1.2. Background

A number of observational (Subsection 1.2.1) and modeling (Subsection 1.2.2) studies provide useful background for this study and are cited below.

1.2.1. Observational Studies

The CB is the largest estuary that drains into the Middle-Atlantic Bight (Beardsley and Hart, 1978). To a first approximation, CB is a

[2]From this point on, we refer to the Scanning Low-Frequency Microwave Radiometer as the salinity mapper.

two-layer system with the upper layer discharging low salinity water onto the shelf, while the lower layer takes in higher salinity water from the adjacent shelf. Near the bottom, observations (Boicourt, 1973) indicate that CB takes in water over an alongshore band of the order of 30 km in width. The distribution of salinity within CB tends to be oblique with higher salinities on the eastern side and lower salinities on the western side, consistent with the fact that most of the "freshwater" discharge originates on the western side of the Bay. In a recent study on the effects of bathymetry in determining the transport of water and salt across the entrance of CB, Valle-Levinson and Lwiza (1995) found that the depth-averaged mean longitudinal flow into the Bay occurred over the deep navigational channels, and outflow occurred over the shoals on either side of the channels. Near the mouth of the Bay, hydrographic data indicate that the vertical stratification is primarily controlled by salinity (Boicourt, 1973), and, as a result, the horizontal circulation is likewise expected to be primarily determined by the distribution of salinity. The low salinity core of the plume which emanates from the mouth of the bay tends to overlie the deep channel located on the south side of the bay mouth that extends offshore and turns to the southeast (Holderied and Valle-Levinson, 1997). The buoyant plume of low salinity water is deflected south past Cape Henry by the Coriolis force and forms a southward-flowing coastal current. According to Boicourt (1973), this coastal current has the characteristics of a quasi-geostrophic jet. The area covered by the plume expands and contracts in direct response to discharge from the Bay (*e.g.*, Thomas, 1981).

Three of the primary factors that determine the outflow from CB are river discharge or buoyancy forcing, wind forcing, and tidal rectification over the shoal which separates the two channels located at opposite sides of the bay entrance (Valle-Levinson *et al.*, 1997). The circulation of the shelf waters off the mouth of the Bay varies with changes in discharge from the Bay, the local winds, and to a lesser extent, stratification (Norcross and Stanley, 1967). According to Goodrich (1987), both gravitational and meteorological forcing contribute to the nontidal exchange across the mouth of CB. Under typical conditions, the CB plume extends offshore several tens of km or more. The plume may extend southward along the coast as far south as Cape Hatteras, particularly after extreme events such as Tropical

Storm Agnes (Boicourt, 1973). At the offshore boundary of the plume, a sharp salinity front often occurs. Tidal variability associated with the outflow from CB is significant and is primarily due to the semidiurnal constituent (*e.g.*, Valle-Levinson *et al.*, 1997; Beardsley and Hart, 1978). According to Ruzecki *et al.* (1976), the plume expands and contracts on tidal time scales in accordance with the ebb and flood tides, respectively. Following Tropical Storm Agnes, the distribution of flood waters on the shelf indicated that pulses of low-salinity water left the Bay during the ebb tide and were separated from one another by intrusions of high-salinity shelf water on the flood tide (Kuo *et al.*, 1976).

The location of the plume is also affected by the local winds and the circulation on the shelf. Winds from the southwest tend to disperse and extend the plume, especially during ebb tide (Munday and Fedosh, 1981), and allow it to move further offshore before turning south along the coast (Holderied and Valle-Levinson, 1997). Winds from the north-northeast act to constrain the plume by keeping it close to the coast south of the mouth. Consistent with the results of Munday and Fedosh, Boicourt *et al.* (1987) found that downwelling-favorable winds suppressed the seaward excursion of the plume near the mouth, but intensified the coastal jet further downstream. On the other hand, upwelling-favorable winds caused the plume to spread seaward away from the coast. Increased stratification may also extend the influence of bay waters further offshore (Boicourt, 1981).

1.2.2. Modeling Studies

Using a simple one layer model, Beardsley and Hart (1978) found that CB draws in water from a relatively wide alongshore band, of the order of 30 km, in general agreement with the observations of Boicourt (1973). In a series of modeling studies which employed a three-dimensional, primitive equation model, Chao and Boicourt (1986), and Chao (1988a and b; 1990), showed how the winds, tides, and river discharge, plus other factors affect the local circulation for mid-latitude estuarine/shelf environments such as CB. Chao and Boicourt (1986) showed that plume-induced circulations derive their energy primarily from the release of potential energy associated with river discharge which produces pressure gradients that spread the plume

seaward. The Coriolis force was apparent in deflecting both the plume itself to the right, as well as the local wind-driven surface currents. They also found that the loss of mass in the upper layer of the plume through detrainment should be taken into account in order to generate plumes that are more realistic further offshore.

Chao (1988a) showed the importance of lateral asymmetries in the circulation of a river-forced estuary. He further presented a classification scheme for river-forced plumes that relate the Froude number to a dimensionless parameter indicating the amount of dissipation that occurs. Chao (1988b) showed that the primary effect of wind forcing on estuarine plumes over the shelf is to produce surface Ekman drift. For downwelling-favorable winds, an elongated coastal jet occurs in the downwind direction. For cross-shelf winds, the nearshore Ekman drift is retarded by sea level setup or setdown. Chao (1990) demonstrated that a three-dimensional model which included forcing from the semidiurnal tide resulted in a residual circulation that included two counter-rotating eddies off the mouth of the estuary. Although these eddies enhanced plume growth in the near-field, they retarded the development of the coastal jet in the far-field.

Wang and Kravitz (1980) showed that the initial injection speed of waters discharged from an estuary onto the shelf has only a small effect on the circulation induced within the plume itself. This conclusion was further supported by the model studies of Chao and Boicourt (1986). Zhang *et al.* (1987) used an analytical model together with observations to examine the behavior of three different river plumes including the CB plume. Unlike many other studies, Zhang *et al.*, emphasized the importance of the prevailing alongshore flow in determining the directionality of the plumes. For CB, their model results indicated that bottom steepness is an important factor in influencing flow characteristics of the plume beyond the mouth of the Bay.

Using a layer model, Garvine (1987) demonstrated that plumes which are affected by earth rotation initially develop fronts along their outer boundary. As further development takes place, the plume turns toward the coast under the influence of the Coriolis effect, and, finally, a coastal current develops further downstream. Using a primitive equation model, Weaver and Hsieh (1987) found that when fresh water was released from a mid-latitude estuary onto the continental shelf, a first baroclinic-mode Kelvin wave propagated into the estuary,

and along the continental shelf in the direction of a coastal trapped wave. Numerical techniques developed by O'Donnell (1990) were employed in a model to investigate the unsteady behavior of small-scale river plumes. He found that tidally-reversing crossflows diluted the plume through vertical mixing immediately following high and low tides.

Oey and Mellor (1993) examined the evolution and variability of an estuarine plume, and its associated coastal front and coastal current. The plume and front were found to be unsteady with a period of 5–10 days. The plume pulsated and coastal currents propagated down the coast intermittently. Wheless and Klinck (1995) examined the evolution of buoyancy-driven flow over a sloping bottom using a two-dimensional, vertically-averaged numerical model. They found that the interaction of horizontal density gradients and a sloping bottom led to vortex stretching, cross-isobath flow, and the development of a cyclonic gyre further offshore, following outflow from a coastal estuary of dense, winter-like waters from a point source. Using the Princeton Ocean Model (Blumberg and Mellor, 1987) with a horizontal resolution of 0.25 km, Wheless and Valle-Levinson (1996), examined the exchange between an estuary and a sloping shelf through a narrow inlet. Buoyancy forcing and the semidiurnal tides were included. A radially spreading buoyant plume was formed over the shelf with strong anticyclonic flow along the front. Two tidally-induced asymmetric eddies were formed, one on each side of the inlet, which strongly influenced the circulation locally, reminiscent of the results obtained by Chao (1990).

The modeling studies referenced above have provided guidance for the present study. However, this study is unique because it incorporates all of the primary forcing elements that affect the behavior of the CB plume including the tides, winds, and river discharge within the framework of a realistic ocean forecast system.

2. THE COASTAL OCEAN FORECAST SYSTEM

The Coastal Ocean Forecast System is being developed by the National Weather Service, the National Ocean Service, and Princeton University to provide a regional ocean forecasting capability for U.S. coastal

direction of a coastal trapped
ed by O'Donnell (1990) were
ne unsteady behavior of small-
lly-reversing crossflows diluted
ediately following high and low

evolution and variability of an
astal front and coastal current.
unsteady with a period of 5–
stal currents propagated down
l Klinck (1995) examined the
r a sloping bottom using a two-
erical model. They found that
gradients and a sloping bottom
flow, and the development of
owing outflow from a coastal
rom a point source. Using the
d Mellor, 1987) with a horizon-
nd Valle-Levinson (1996), ex-
ry and a sloping shelf through a
the semidiurnal tides were in-
plume was formed over the shelf
the front. Two tidally-induced
on each side of the inlet, which
cally, reminiscent of the results

ove have provided guidance for
y is unique because it incorpo-
ents that affect the behavior of
s, and river discharge within the
st system.

CAST SYSTEM

being developed by the National
ervice, and Princeton University
ing capability for U.S. coastal

waters on an operational basis. It is based on the Princeton Ocean Model, a three-dimensional ocean circulation model (*e.g.*, Blumberg and Mellor, 1987). This model is based on the primitive equations, employs a free upper surface, and has a second order turbulent closure submodel to parameterize mixing (Mellor and Yamada, 1982). COFS at the present time produces 24-hour forecasts of temperature, salinity, the three components of velocity, and surface elevation. COFS is coupled to the National Centers for Environmental Prediction's (NCEP's) high resolution ETA regional atmospheric forecast model (Black, 1994) which provides surface fluxes of heat, moisture and momentum at three-hour intervals. Coupling between the atmosphere and ocean is one-way which has generally proven to be satisfactory for real-time forecasting.[3] The model is reinitialized every 24 hours with the previous day's forecast. The U.S. Navy's Generalized Digital Environmental Model (GDEM; Teague *et al.*, 1990) is used to provide the model's initial conditions for temperature and salinity when it is initially spun up from rest. The current version of COFS includes astronomical tidal forcing along the open boundaries and body forcing within the model domain for six tidal constituents (Chen and Mellor, 1998). The model is driven along its open boundaries with climatological estimates of temperature and salinity from GDEM, and constant volume transport which is specified separately.

Fresh water inputs are specified for 16 rivers, bays and estuaries along the U.S. East Coast and are based on monthly climatological data (Blumberg and Grehl, 1987; Koutitonsky and Bugden, 1991). In the model, the outflow from CB (and the other rivers, bays and estuaries within the model domain) is specified as a volume flux from a single grid point (*i.e.*, a point source) located at the mouth of the Bay at 37.02°N, 76.05°W (P. Chen, 1998, personal communication). A salinity of zero psu and an injection velocity of zero are initially assigned to the outflow.[4] This fresh water is mixed with saline water from the previous time step in the surrounding grid cell to produce water

[3]One exception is for hurricanes, and, as a result, two-way coupling may be implemented in the future.

[4]The assignment of zero velocity to the water discharged from CB is consistent with the results of Wang and Kravitz (1980) and Chao and Boicourt (1986) who both indicated the importance of the potential energy associated with the plume, and not its kinetic energy in influencing its behavior over the shelf.

of lower salinity. The lower salinity is calculated according to

$$S_t(x,y,z) = S_{t-1}(x,y,z) - S_{t-1}(x,y,z) * VF_t * (2.0 + D_i/H + D_{i+1}/H) * (2.0 * \Delta T)/A(x,y) * D_i$$

where S is the salinity at time steps t and $t-1$ for location x, y, and z, VF_t is the volume flux in m^3/sec at time t, D_i is the ith depth, H is the bottom depth, ΔT is the internal model time step, and A is the area of one grid cell. The outflow is distributed vertically so as to provide a linear decrease with depth. This is accounted for above by the term $(2.0 + D_i/H + D_{i+1}/H)$. If the mean outflow, Q_m, is assigned to the middle of the volume, then the flow at the surface is approximately $2 * Q_m$, and the flow at the bottom is approximately equal to zero.

The model employs a terrain-following sigma coordinate system in the vertical, and a curvilinear grid in the horizontal. The model has 18 layers with increased vertical resolution in the mixed layer and the upper thermocline. The spatial resolution increases from 20 km offshore to 10 km near the coast. The coastal boundary corresponds to the 10 m isobath. A no-slip boundary condition is employed at the coast which produces a boundary layer whose thickness is less than one half the distance between grid points. Because the Arakawa C staggered grid system is used in the model (O'Connor, 1991), the velocity components are zero on the coastal boundary, and the nearest non-zero velocities are one-half grid cell away from the coast. The model bathymetry is based on the U.S. Navy's digital bathymetric database with 5-minute resolution (DBDB-5) and 15-second resolution digital data from the National Ocean Service over the shelf. Finally, ocean data assimilation is underway and uses *in situ* SSTs and satellite retrievals of SST from the Advanced Very High Resolution Radiometer. Ongoing evaluations of COFS which include data assimilation have shown significant improvement in model performance over model runs without data assimilation (Kelley *et al.*, 1997).

3. THE SCANNING LOW-FREQUENCY MICROWAVE RADIOMETER

The ability to measure surface salinity over the ocean can be traced back to at least 1977 when Blume *et al.* (1978) estimated sea surface

salinity from microwave measurements of brightness temperature from an airborne radiometer. Kendall (1981) used an L-band microwave radiometer aboard an aircraft to measure surface salinity in the vicinity of the CB plume as part of the Superflux II experiment.

Airborne measurements of surface salinity off the mouth of CB and Virginia Beach have been made on several occasions during the past two years using a recently-developed salinity mapper called the Scanning Low-Frequency Microwave Radiometer. The salinity mapper is an L-band passive microwave radiometer operating at a frequency of 1.413 gHz. The salinity mapper also has a dual-channel infrared radiometer to measure SST which is also required in the measurement of sea surface salinity. For a more detailed description of this instrument and the factors which affect the measurement of sea surface salinity, see Goodberlet *et al.* (1997). Although the instrument's sensitivity to changes in salinity is somewhat limited, it can provide an accuracy of 1 psu, or better, in most coastal areas. The mapper is mounted on a small single-engine aircraft and has the capability to produce maps of surface salinity at the rate of 1000 km^2 per hour with a spatial resolution of 1 km for an aircraft speed of 50 m/sec operating at an altitude of 2.5 km. Recent applications are described in Miller *et al.* (1998).

4. THE EXPERIMENT

Hurricane Fran produced an extreme rainfall event which resulted in greatly increased outflow of low salinity water from the mouth of CB. Data from the salinity mapper were available on two dates (September 14 and 20, 1996) following HF which provided a means of validating our model results at least over the near-field region of the plume domain. We chose the simplest scenario for generating outflows from the Bay which were computed from August 15–September 20, 1996 in response to the river inflows that took place before, during, and following HF. These outflows were generated by summing up the observed streamflows from the U.S. Geological Survey river gages for the nine largest rivers that flow into CB. These account for approximately 93 percent of the surface input into CB. An additional 7 percent was included to account for surface water input from all other sources. Finally, ground water entering the Bay was accounted for by taking 10 percent

of the total surface input and adding it to the total daily surface water input to CB. The resulting discharge function does not take into account the time required for the riverine waters to circulate through the bay system. As a result, the discharge is treated as a single pulse in the outflow which occurs over a period of just a few days in early September following the passage of HF. A more realistic discharge function would have distributed the outflow volume over a much longer period. The resulting discharge function created conditions that were expected to have maximum impact on the model-generated plume. Figure 1 shows the discharge function based on daily values of stream flow together with the discharge time history based on climatology. A volume of water more than ten times greater than the climatological outflow for September was discharged between 6 and 10 September, 1996.

Two model runs were conducted: a control run which used outflows based on the existing climatological data, and a separate hindcast run which used the daily outflows from the discharge function depicted in Figure 1. Both runs were initiated on August 15, 1996, approximately 30 days prior to the period of interest. The model output for each date is valid at 2400 UTC on the day in question. Figure 2 shows the study area and the model grid point locations for all grid points in water depths of 10 m or greater. Surface forcing from the ETA regional atmospheric forecast model was identical for both COFS runs. Three dates were considered in generating plumes of low salinity water off the mouth of CB from COFS: September 8, 14, 20, 1996. The first date corresponds to the time of maximum outflow from CB following HF (Fig. 1 – no corresponding salinity map was available for this date), and the last two dates correspond to times when salinity maps were available.

The two variables of primary interest in this study are salinity and velocity (x and y components) in the top layer of the model.[5] The exact depth of these "surface" variables corresponds to the mid-depth of the top layer in the model. This layer depth, in turn, depends on bottom depth because of the sigma coordinate system which is used. However, near the mouth of CB, it is always less than one meter. To suppress the influence of the tides, the salinities and currents have been daily-averaged.

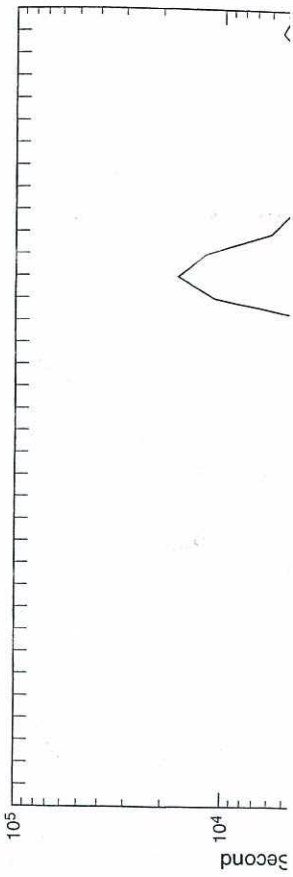

[5]Satellite maps of sea surface temperature (SST) were also examined, but the gradients in SST in the area of interest were less than 0.05°C/km.

g it to the total daily surface
charge function does not take
ne riverine waters to circulate
e discharge is treated as a single
period of just a few days in early
A more realistic discharge func-
w volume over a much longer
created conditions that were ex-
model-generated plume. Figure
on daily values of stream flow
based on climatology. A volume
in the climatological outflow for
nd 10 September, 1996.
control run which used outflows
ata, and a separate hindcast run
e discharge function depicted in
August 15, 1996, approximately
The model output for each date is
on. Figure 2 shows the study area
all grid points in water depths of
the ETA regional atmospheric
OFS runs. Three dates were con-
salinity water off the mouth of
1996. The first date corresponds
CB following HF (Fig. 1 – no
able for this date), and the last
alinity maps were available.
est in this study are salinity and
op layer of the model.[5] The exact
responds to the mid-depth of the
pth, in turn, depends on bottom
system which is used. However,
than one meter. To suppress the
and currents have been daily-

ST) were also examined, but the gradients
05°C/km.

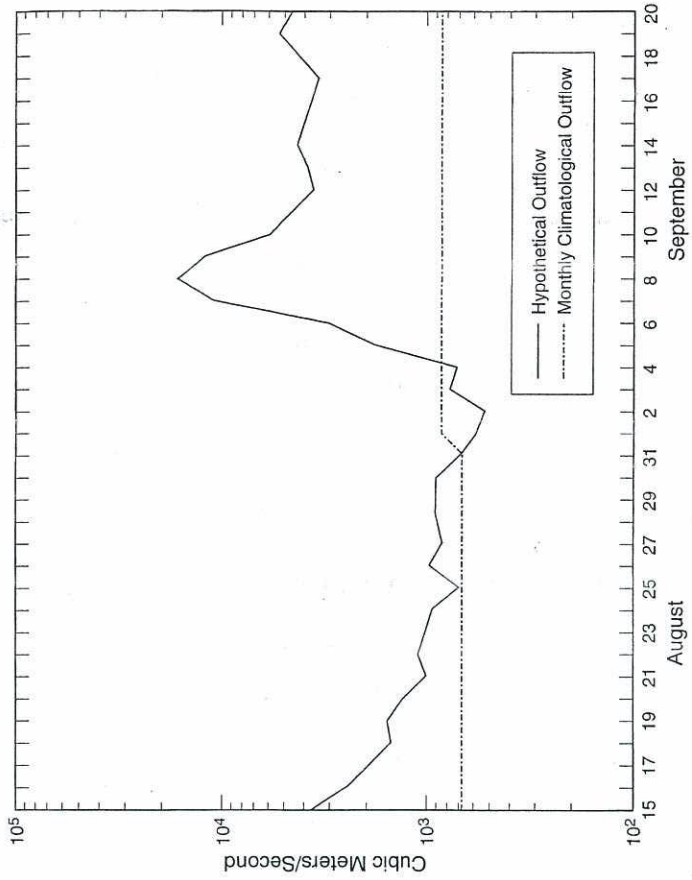

FIGURE 1 Discharge function showing daily volume outflow (solid curve) for Chesapeake Bay from August 15 through September 20, 1996. Details on how the function was computed are given in the text. The monthly climatological outflow employed in the COFS control runs is shown by the dash-dot curve.

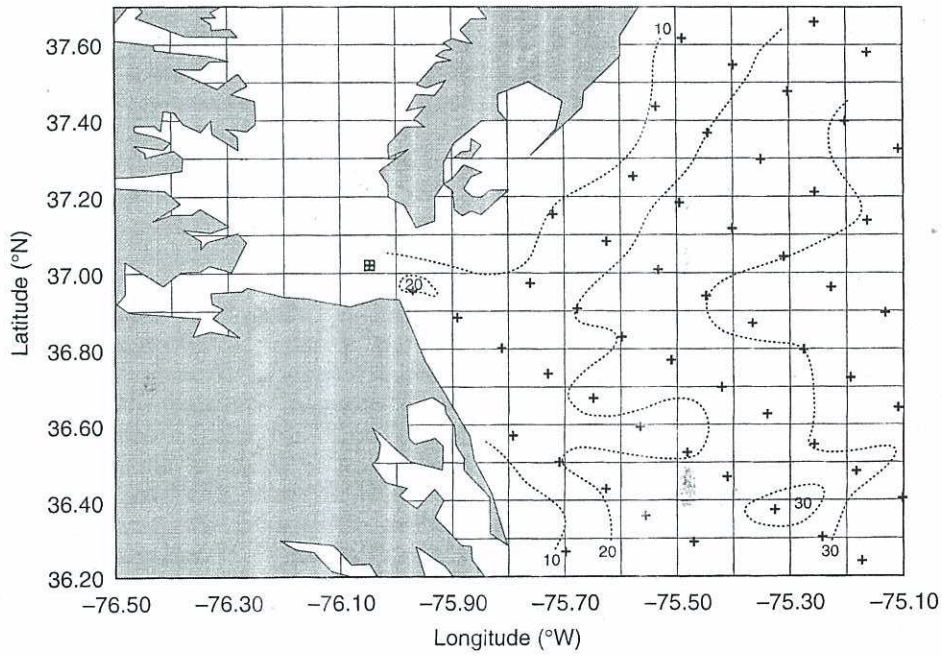

FIGURE 2 Model grid point locations for the study area. Dotted contours indicate bottom depths in meters.

The salinity data use
salinity mapper on two
and 2149 UTC, and S
1996. These data were
which is owned and
Science. The maps of s
shown in Figure 3. Th

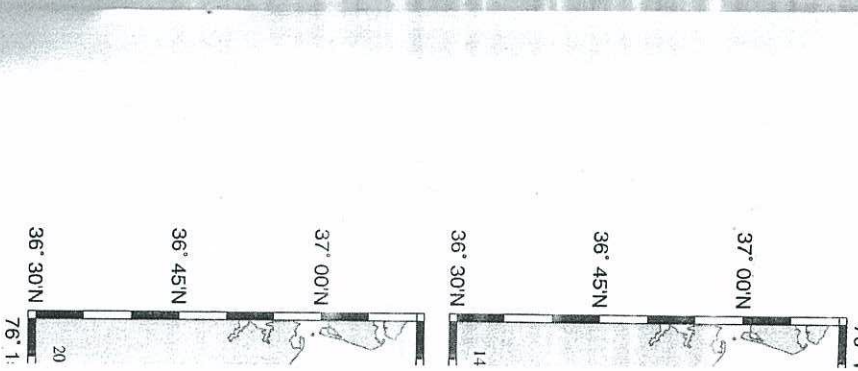

FIGURE 3 Maps of surfa
Microwave Radiometer for S
1996. "CC" refers to Cape
Chesapeake Bay, and "CH
Chesapeake Bay. The distar
15km. Each pixel represents

The salinity data used in this study were acquired with an airborne salinity mapper on two separate dates, September 14th between 1845 and 2149 UTC, and September 20th between 1910 and 2207 UTC, 1996. These data were collected aboard a DeHavilland Beaver aircraft which is owned and operated by the Virginia Institute of Marine Science. The maps of surface salinity produced by this instrument are shown in Figure 3. They were constructed from 10 east-west parallel

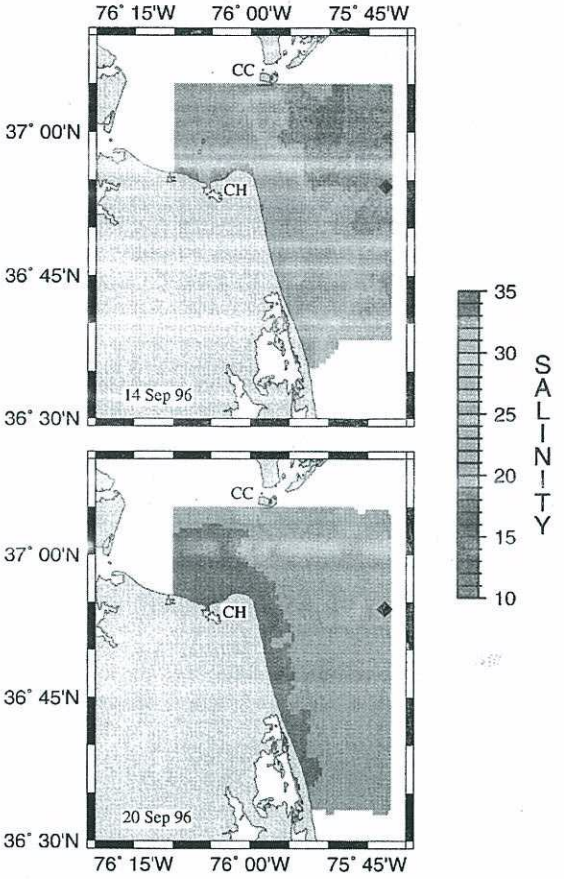

FIGURE 3 Maps of surface salinity obtained from the Scanning Low-Frequency Microwave Radiometer for September 14 (upper panel) and September 20 (lower panel), 1996. "CC" refers to Cape Charles located at the north end of the entrance to Chesapeake Bay, and "CH" refers to Cape Henry located at the south end of Chesapeake Bay. The distance from Cape Charles to Cape Henry is approximately 15 km. Each pixel represents a one km^2 area. (See Color Plate II).

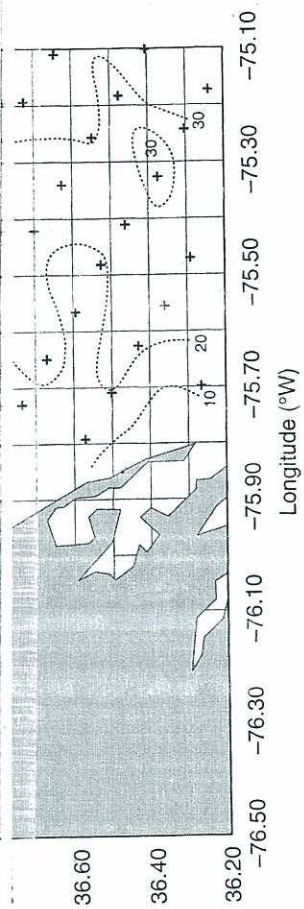

FIGURE 2 Model grid point locations for the study area. Dotted contours indicate bottom depths in meters.

flight lines flown at an altitude of approximately 2.6 km. The area covered was about 2500 km^2 at a spatial resolution on the ground of approximately 1 km.

5. RESULTS

5.1. Plume Characteristics

The results of the model runs for surface salinity, using the climatological outflows (control runs), and the daily outflows (hindcasts) are shown in Figures 4, 5 and 6 for September 8, 14, and 19[6], respectively. The surface salinities are shown in the top panel for the control runs and in the bottom panel for the hindcasts, for each date. Because of the relatively large discharge that was specified for the period between 6 and 10 September, a significant impact on plume structure for the hindcast runs was anticipated. Indeed, in the immediate vicinity of the bay mouth, salinities as low as 10 psu were predicted by the model using the daily discharge function, whereas, the control run only forecasted salinities as low as 28 psu in the same area (Fig. 4). At this early stage, the impact of the anomalous outflow extended out to approximately 50 km offshore. Almost a week later on September 14th, major differences between the two runs are apparent. Salinities as low as 27 psu exited the Bay in the hindcast, while the lowest salinities for waters leaving the Bay in the control run were 31 psu (Fig. 5). Perhaps even more significant is the spatial extent of the low-salinity waters associated with the hindcast which extend almost 60 km offshore out to the position of the 36 psu isopleth. It is important to note that, although the location of the 36 psu isopleth in the model lies this close to shore, in reality, waters with salinities in this range are located considerably further offshore, usually within the Gulf Stream. The reason for this intrusion of higher salinity water off the mouth of CB is due to the fact that the model-generated Gulf Stream tends to follow the bathymetry around Cape Hatteras for a short distance, creating a fictitious meander just north and east of the Cape, rather than separating correctly and

[6]The model output for September 19th was used since it was actually closer to the time when the salinity observations were acquired.

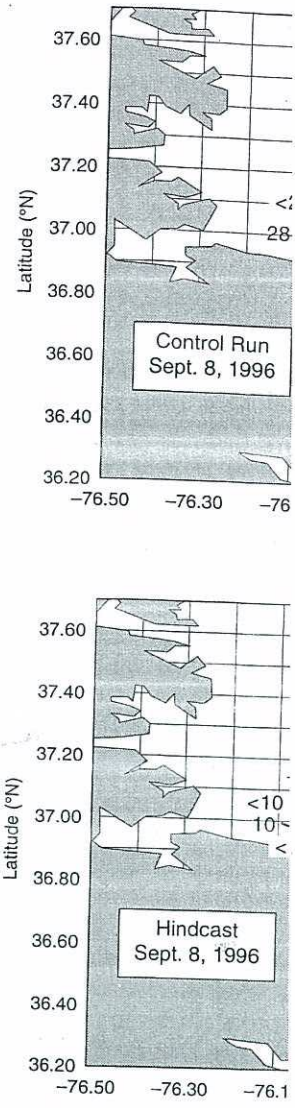

FIGURE 4 Map of surface sali
for September 8, 1996. The top p
monthly climatological outflows
hypothetical discharge function sl

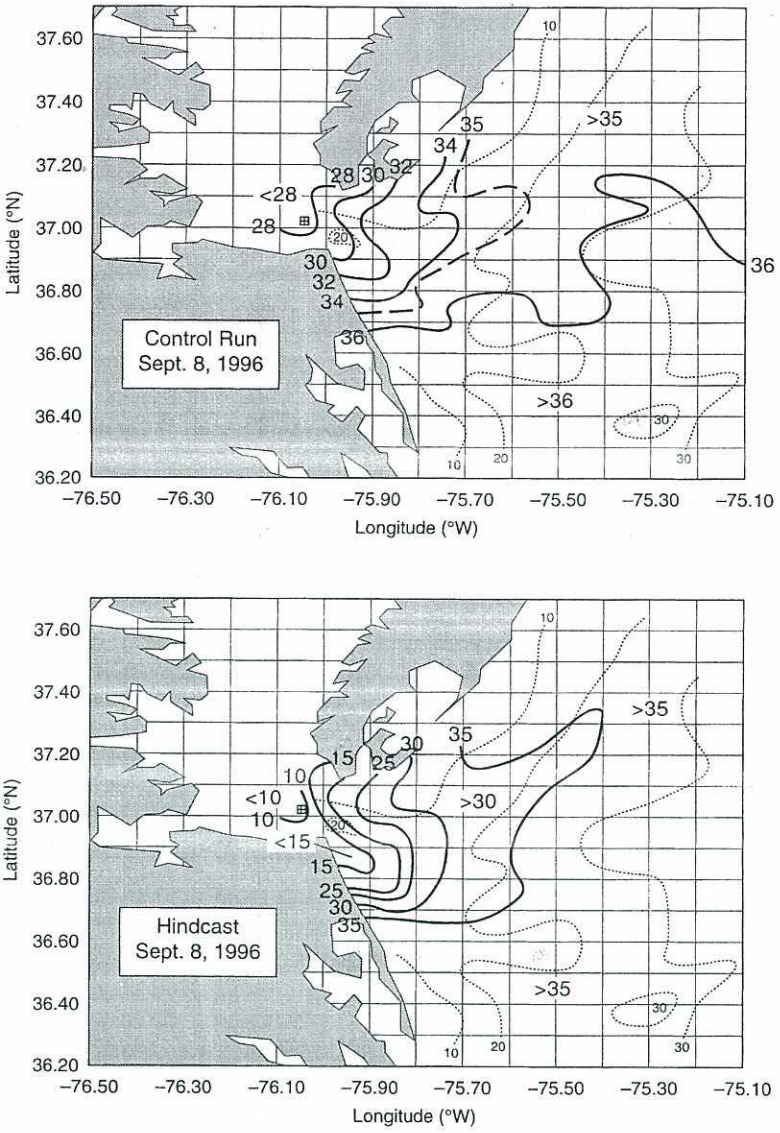

FIGURE 4 Map of surface salinity produced by the Coastal Ocean Forecast System for September 8, 1996. The top panel shows the control run for the model which used monthly climatological outflows for CB, whereas the lower panel employed the hypothetical discharge function shown in Figure 1.

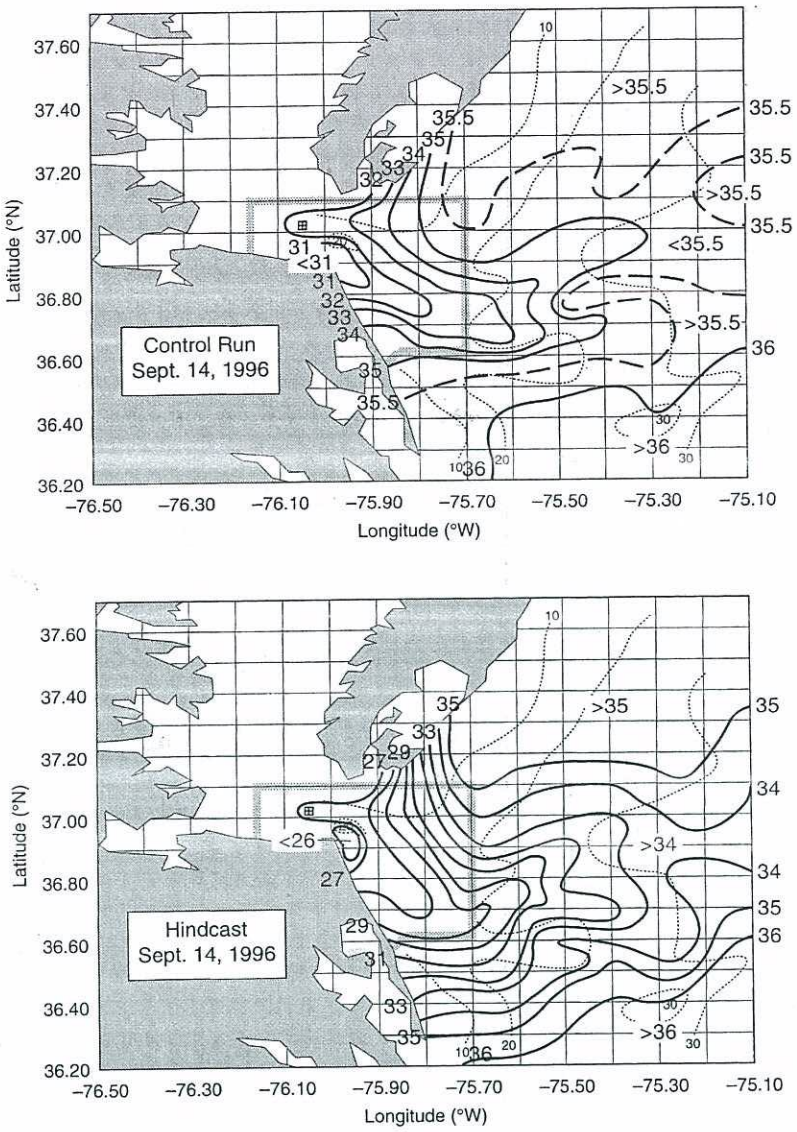

FIGURE 5 Same as Figure 4 except that the date is September 14, 1996. The area enclosed by the box outlined with light thick lines is the area covered by the salinity map for the same date displayed in Figure 3 (upper panel).

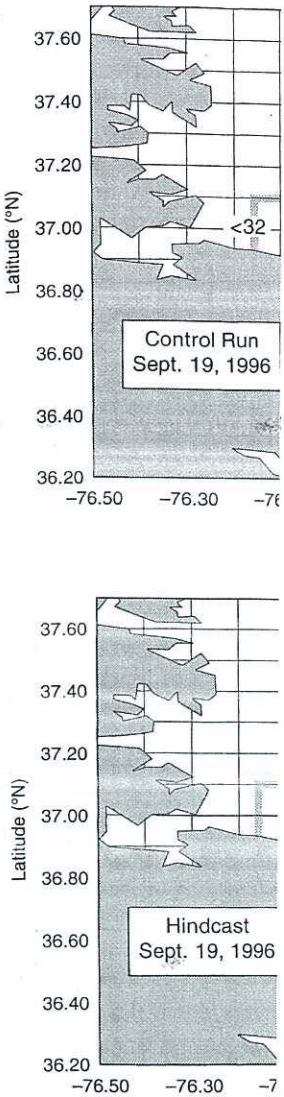

FIGURE 6 Same as Figure
enclosed by the box outlined w
for the same date presented in

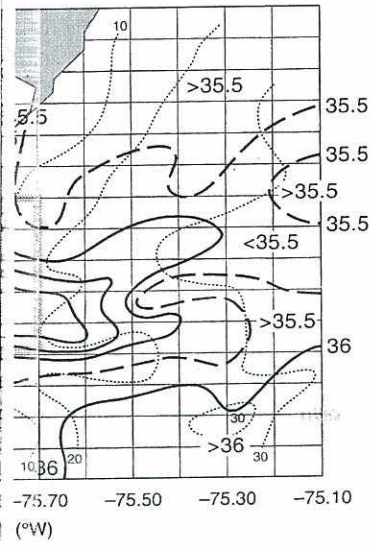

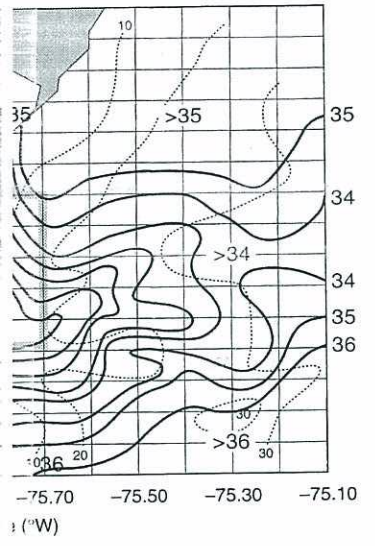

date is September 14, 1996. The area
es is the area covered by the salinity map
panel).

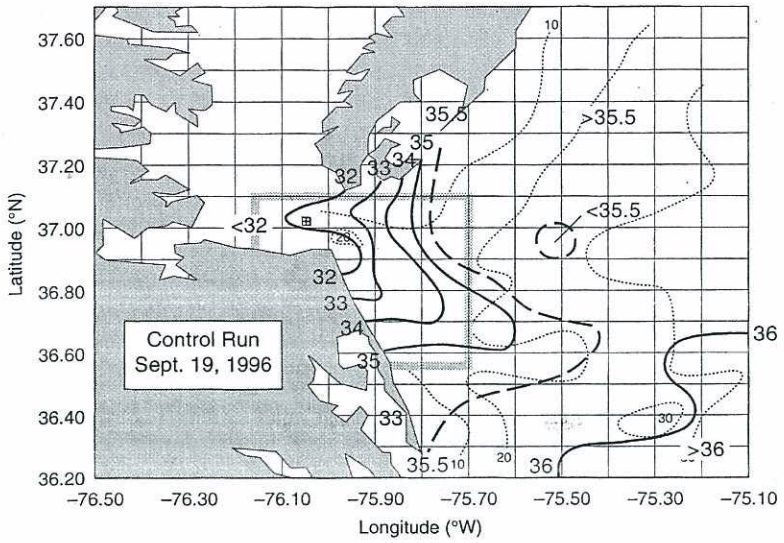

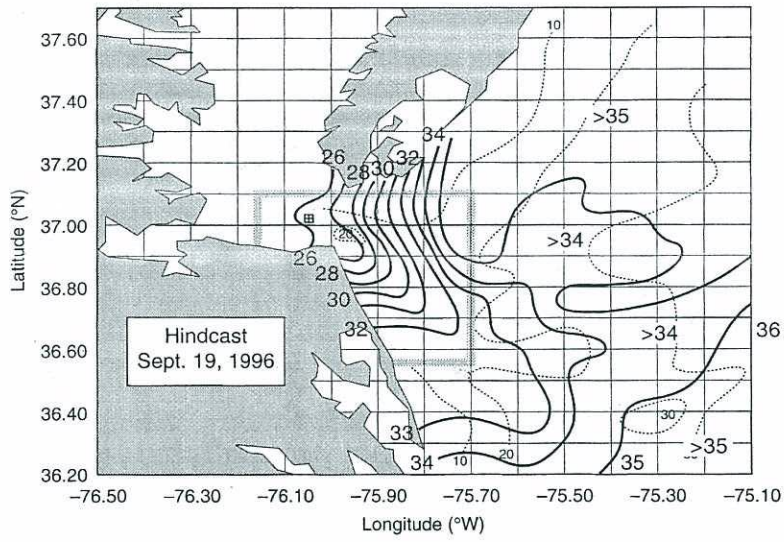

FIGURE 6 Same as Figure 5 except that the date is September 19, 1996. The area enclosed by the box outlined with light thick lines is the area covered by the salinity map for the same date presented in Figure 3 (lower panel).

flowing directly offshore at this location. Although this problem is apparently common to other ocean circulation models (Dengg *et al.*, 1996), it has recently been corrected to some extent in COFS through the assimilation of satellite-derived SSTs (Kelley *et al.*, 1997).

Although the plume initially follows the coast south of Cape Henry, further offshore it turns cyclonically to the northeast. This curvature, which is evident in both runs, is particularly apparent in the hindcast. A weak low-pressure system moved through the area on 12 September with wind speeds of up to 14 m/sec generally from the south and may have contributed to a greater offshore transport of water and cyclonic rotation of the plume. The axis of the plume in the hindcast extends south of Cape Henry to approximately 36.6°N and is located roughly 10 km offshore. According to the observations of Boicourt *et al.* (1987) and the model results of Chao (1988b), winds from the south (*i.e.*, upwelling-favorable) cause the plume to spread seaward due to the influence of Ekman transport. These results are also in general agreement with past observations in this area acquired during periods of high seasonal outflow from the Bay (Ruzecki, 1981). Also, the additional waters which were discharged onto the shelf in the hindcast, sharply increased the salinity gradients in several locations favoring frontal intensification, *i.e.*, frontogenesis, locally. Comparisons of the model-generated salinities near Cape Henry just inside the Bay and near the coast south of Cape Henry (Fig. 5), with observed salinities from the salinity mapper, show that the salinities from the hindcast ($\sim$26 psu) are much closer to the observed salinities ($\leq$20 psu) than are the salinities from the control run in this area ($\sim$31 psu). Also, the stronger gradients indicated in the hindcast appear to be generally more consistent with the gradients observed in the data from the salinity mapper than are the gradients produced in the control run. The actual gradients from the salinity mapper for the 14th were as high as 1.4 psu/km northeast of Cape Henry compared to gradients as high as 0.5 psu/km from the model hindcast in the same area. Because the spatial resolution of the model is approximately 10 km in this region (Fig. 2), the strength of the gradients from the model were not expected to match the gradients estimated from the salinity mapper which has a resolution in the neighborhood of 1 km.

The shape of the plume in the hindcast changed from the 14th to the 19th (Fig. 6), and the offshore extent was somewhat reduced. The axis

ation. Although this problem is
circulation models (Dengg *et al.*,
to some extent in COFS through
STs (Kelley *et al.*, 1997).
s the coast south of Cape Henry,
to the northeast. This curvature,
icularly apparent in the hindcast.
hrough the area on 12 September
erally from the south and may
e transport of water and cyclonic
he plume in the hindcast extends
ely 36.6°N and is located rough-
observations of Boicourt *et al.*
o (1988b), winds from the south
plume to spread seaward due to
These results are also in general
this area acquired during periods
ay (Ruzecki, 1981). Also, the ad-
ed onto the shelf in the hindcast,
nts in several locations favoring
nesis, locally. Comparisons of the
e Henry just inside the Bay and
(Fig. 5), with observed salinities
t the salinities from the hindcast
bserved salinities (≤ 20 psu) than
n in this area (~ 31 psu). Also, the
hindcast appear to be generally
observed in the data from the sa-
produced in the control run. The
napper for the 14th were as high
nry compared to gradients as high
ast in the same area. Because the
pproximately 10 km in this region
nts from the model were not ex-
ted from the salinity mapper which
d of 1 km.
dcast changed from the 14th to the
t was somewhat reduced. The axis

of the plume, rather than turning cyclonically, more-or-less parallels the coast. The plume structure for the control run indicates contractions particularly for isopleths between 32 and 35 psu where forcing due to volume flux at the mouth was maintained at a constant level (Fig. 1). Thus, based on past observations and model results, the effects of surface wind forcing should also be considered. On September 17th, a second, deeper low-pressure system moved through the area with maximum wind speeds of at least 17 m/sec which were initially from the south and then shifted to the northwest on the 18th. Because the wind direction changed significantly during the passage of this low-pressure system, the net effect of the winds is not intuitively clear. However, the model results suggest that the overall effect of the winds may have been to constrain the development of the plume at least between the 14th and 19th of September. Boicourt *et al.* (1987) found that northerly winds suppressed the seaward development of the plume close to the mouth of CB, whereas, southerly winds caused the plume to spread seaward. Our results are generally consistent with this interpretation. A comparison of the salinity maps from the salinity mapper with the model-generated salinity maps for the 19th again shows that the salinities from the hindcast near Cape Henry just inside the Bay and further south along the coast are much closer to the observed salinities than are the salinities from the control run. Neither the salinities of the hindcasts, nor those of the control runs changed appreciably from the 14th through the 19th near the bay mouth, while the observed salinities near Cape Henry were significantly lower on the 19th (10–15 psu) than they were on the 14th (15–20 psu). Observed salinities on the 19th are not only lower near Cape Henry, but are at least 5 psu lower offshore over most of the region that was mapped. These lower salinities on the 19th may reflect the increasing influence of the freshwater outflow which resulted from HF. This decrease in surface salinity between the 14th and the 19th is not obvious in the model hindcast runs, even though the hypothetical discharge function shows a slight increase in outflow (from $\sim$3400 to $\sim$5400 m^3/sec) between 17th and 19th September. On the 19th, the low salinity plume extends much further south along the coast in the hindcast than it does in the control run ($\sim$40 km further south for the 34 psu isopleth), and, as a result, is more consistent with the observed data. As on the 14th, the stronger gradients in the hindcast compared to the control run on

the 19th are again in better agreement with the salinity gradients in the observed data from the salinity mapper. On this occasion, actual gradients from the salinity mapper northeast of Cape Henry are of the order of 1.4 psu/km, and from the model are again only as high as 0.5 psu/km.

5.2. Model-generated Currents

Model-generated surface currents for the 8th, 14th, and 19th of September are shown in Figures 7, 8 and 9, respectively. As indicated earlier, these currents were daily-averaged to reduce the impact of the astronomical tides. For each date, the panel in the upper left shows the results from the control run, the panel in the upper right, the results from the hindcast, and below, the vector difference (hindcast minus control). As stated in Section 2, the coastal boundary for the velocity components is located approximately 5 km seaward of the coastal boundary in the model, *i.e.*, the 10 meter isobath. The currents for September 8th (Fig. 7) are on the order of 30 cm/sec and clearly directed to the northeast for both model runs. Winds at the C-Man station located approximately 30 km off the mouth of the Bay were consistently from the southwest (200 – 210°) for most of the day and, thus, primarily responsible for producing the observed patterns of flow in the model, allowing for 10° – 15° of rotation to the right due to the Coriolis force. The difference pattern indicates the impact of outflow from the Bay at the three successive grid points nearest the mouth with a maximum speed of 25 cm/sec directed to the southeast. On September 14th (Fig. 8), the model-generated currents generally flow to the southeast with speeds of 15 – 30 cm/sec in response to winds which were consistently from the northwest. South of about 37°N, the direction of surface flow changes more to the south reflecting the influence of the circulation associated with the plume itself. The difference plot reveals four current vectors which overlie the area where the salinity gradient is a maximum. Although the direction of flow here may be unexpected, it is probably due to the fact that the model-generated plume does not lie against the coast, but is located further offshore, allowing return flow to develop along its southern flank. The model-produced currents on the 19th of September (Fig. 9) indicate surface flow to the south at speeds of 15 – 30 cm/sec. Again, the primary influence appears to be from the winds

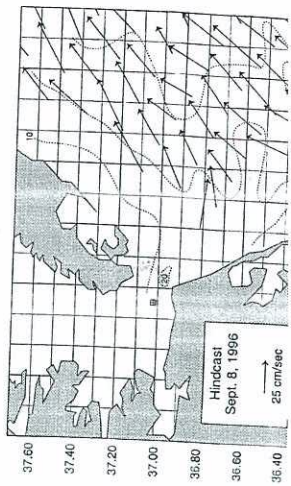

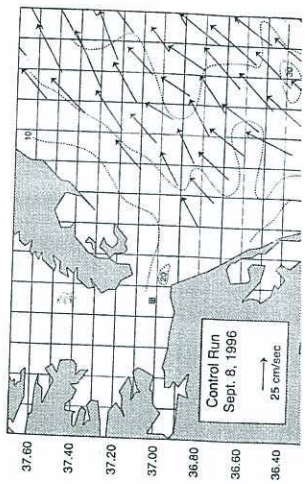

ith the salinity gradients in the
. On this occasion, actual gra-
ast of Cape Henry are of the
del are again only as high as

he 8th, 14th, and 19th of
d 9, respectively. As indicated
ed to reduce the impact of the
anel in the upper left shows the
in the upper right, the results
tor difference (hindcast minus
astal boundary for the velocity
5 km seaward of the coastal
eter isobath. The currents for
of 30 cm/sec and clearly direct-
is. Winds at the C-Man station
uth of the Bay were consistently
t of the day and, thus, primarily
l patterns of flow in the model,
right due to the Coriolis force.
pact of outflow from the Bay at
st the mouth with a maximum
heast. On September 14th (Fig.
rally flow to the southeast with
winds which were consistently
°N, the direction of surface flow
the influence of the circulation
fference plot reveals four current
salinity gradient is a maximum.
ay be unexpected, it is probably
ed plume does not lie against the
allowing return flow to develop
roduced currents on the 19th of
w to the south at speeds of 15–
ce appears to be from the winds

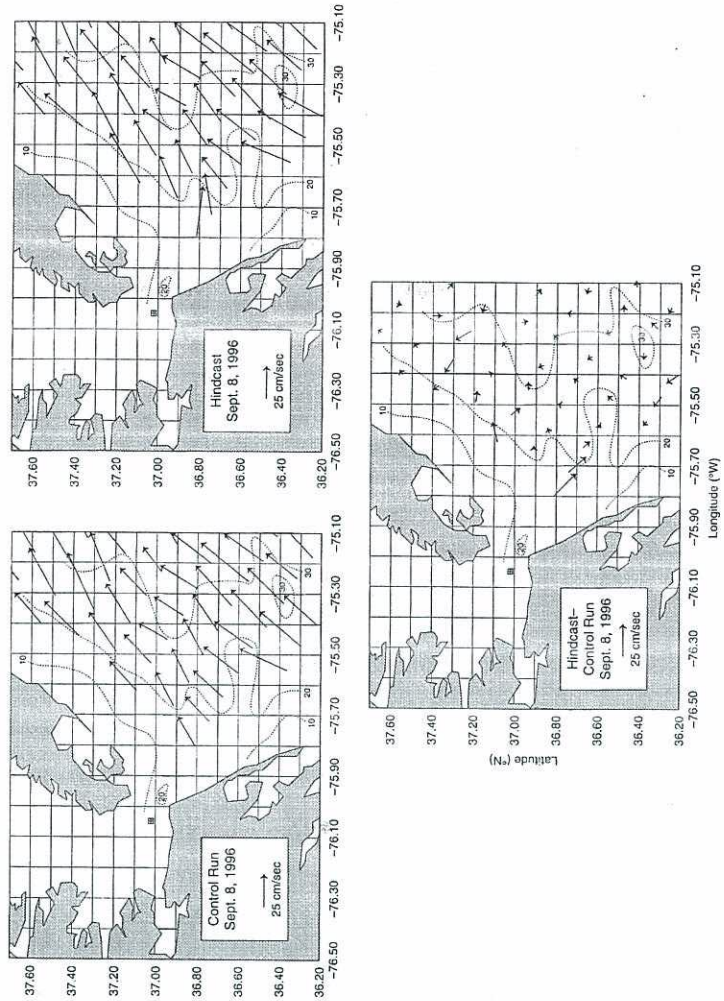

FIGURE 7 Surface currents from the Coastal Ocean Forecast System for September 8, 1996. Results from the control run (upper left) were obtained using monthly climatological outflows for Chesapeake Bay. The hindcast results (upper right) were obtained using a hypothetical discharge function based on a simple summation of the daily observed river inputs to the Bay. The vector difference between the hindcast and the control run are shown below.

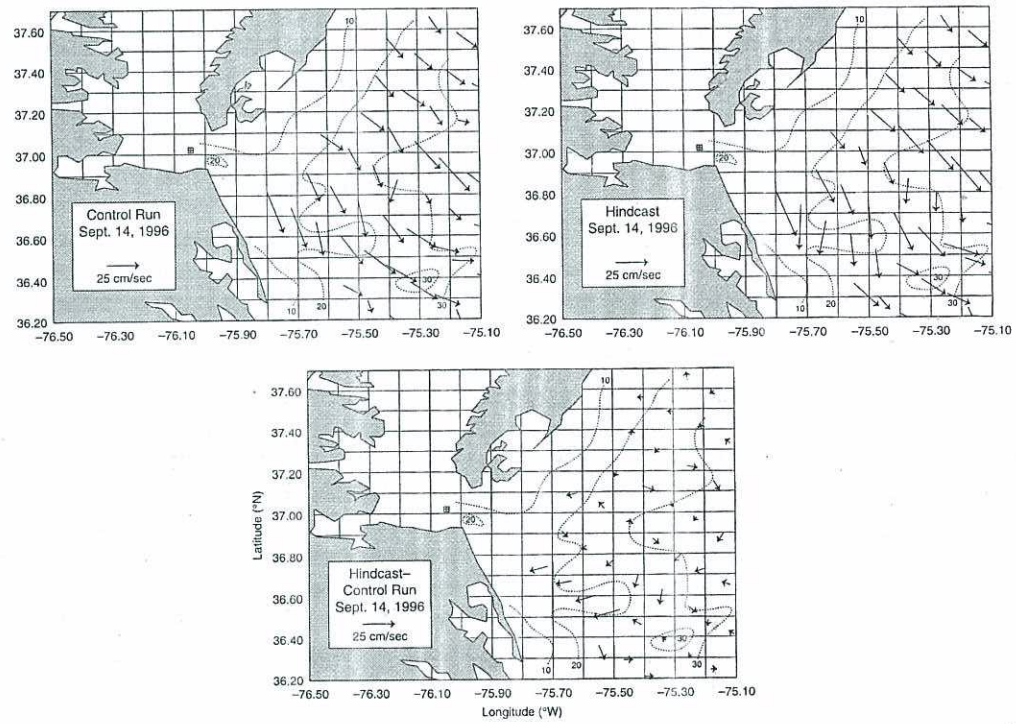

FIGURE 8 Same as Figure 7 but for September 14, 1996.

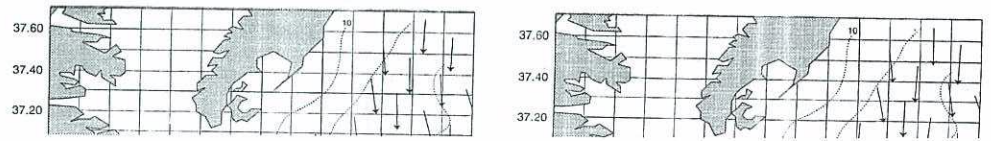

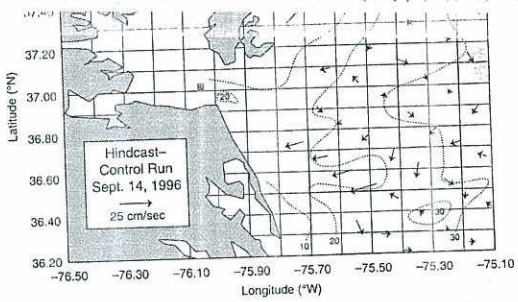

FIGURE 8 Same as Figure 7 but for September 14, 1996.

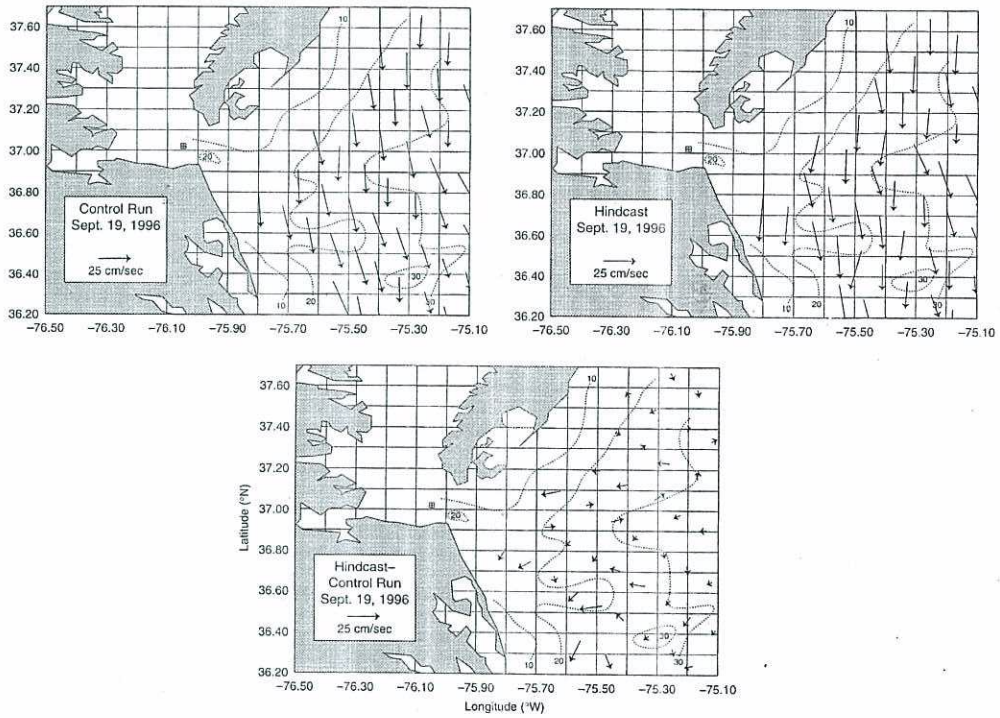

FIGURE 9 Same as Figure 8, but for September 19, 1996.

which were from the north-northwest, allowing for slight, Coriolis-induced rotation. The difference map again shows several current vectors whose locations and direction suggest the influence of the strong salinity gradients associated with the plume. By differencing the control run and the hindcast, we have removed those elements which are common to both fields, which certainly include the effects of wind forcing, but have also removed any effects due to salinity forcing which were common to both fields. Thus, our attempt to separate the effects of wind and salinity forcing are most likely not complete. In any case, the importance of wind forcing on the surface flow is clearly apparent. These results are in good agreement with the effects of wind forcing contained in the observational results of Boicourt *et al.* (1987) and in the model results obtained by Chao (1986b). However, the impact of salinity forcing due to the strong salinity gradients in the region surrounding the plume is also evident, but not as obvious as the impact of wind forcing.

5.3. Subsurface Salinities from the Model

The primary emphasis so far has been on the surface manifestation of the low salinity plume that emanates from CB. Here, we examine the subsurface structure of the low salinity plume by displaying a sequence of 8 vertical profiles of salinity from COFS along a line of model grid points that is closely aligned with the axis of the plume (Fig. 10). Profile sequences for the 14th and 20th of September are displayed for both the hindcast (solid) and the control run (dotted). The average distance between profiles is 10.6 km, and the profile furthest offshore (profile 8) is approximately 75 km from the mouth of the Bay. Although the individual profiles vary significantly, there is a tendency for the strength of the halocline to weaken and the depth of the halocline to become shallower as we proceed offshore. The location of the halocline provides an indication of the depth that effectively separates the plume from the waters below. Based on all of the profiles shown (both dates), this depth appears to be a maximum of about 10 m near the mouth, but further offshore generally shoals to a depth of 5 meters or less. Detrainment or the loss of mass from the plume to the waters below may contribute to the gradual decrease in plume

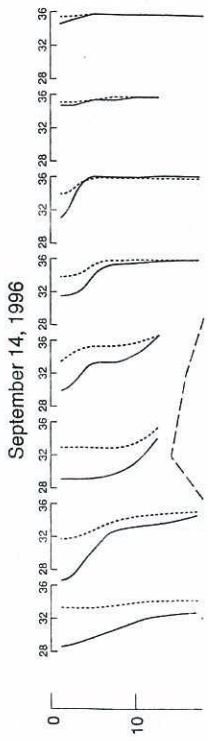

llowing for slight, Coriolis-
in shows several current vec-
st the influence of the strong
ıe. By differencing the control
ıose elements which are com-
le the effects of wind forcing,
ɔ salinity forcing which were
to separate the effects of wind
t complete. In any case, the
ace flow is clearly apparent.
h the effects of wind forcing
Boicourt *et al.* (1987) and in
36b). However, the impact of
y gradients in the region sur-
ot as obvious as the impact of

el

n the surface manifestation of
ɔm CB. Here, we examine the
lume by displaying a sequence
)FS along a line of model grid
axis of the plume (Fig. 10).
h of September are displayed
ıtrol run (dotted). The average
ıd the profile furthest offshore
om the mouth of the Bay.
gnificantly, there is a tendency
veaken and the depth of the
ɔceed offshore. The location of
of the depth that effectively
ow. Based on all of the profiles
s to be a maximum of about
ɔre generally shoals to a depth
loss of mass from the plume to
he gradual decrease in plume

FIGURE 10 A sequence of eight vertical salinity profiles extending along a line from the mouth of CB out to a distance of 74 km offshore for September 14th (upper sequence) and September 20th (lower sequence), 1996. This line corresponds approximately with the major axis of the CB plume. For each location, profiles from both the control run (usually of higher salinities) and the hindcast (usually of lower salinities) are included. The location of each profile is shown in the inset below.

thickness proceeding offshore (Chao and Boicourt, 1986). These model-generated halocline depths agree with plume depths inferred from *in situ* salinity data acquired beyond the mouth by Ruzecki (1981) where plume thicknesses varied from 5–8 m. On the 20th, the three profiles closest to the mouth indicate much lower salinities down to 10 m than the corresponding profiles on the 14th and may reflect the influence of the additional fresh water discharge that is indicated in Figure 1 between the 17th and 19th of September. However, further offshore, profiles on the 20th indicate slightly higher salinities within the plume at least out to the last two profiles. Major differences occur in the profiles between the hindcasts and the control runs for both dates near the mouth where the influence of the higher discharge associated with the hindcast is apparent, but these differences decrease further offshore and almost disappear for profiles 7 and 8.

Overall, the results indicate that (1) COFS has reproduced essential features associated with the CB plume, including its preferred location, length scales, evolution, and variability particularly for cases where the plume lies offshore in response to southerly winds, (2) major differences in plume structure occur using the daily *versus* the climatological discharge functions, including stronger salinity gradients along the periphery of the plume, (3) the structure of the plume responds quickly to rapid changes in volume flux at the mouth of the Bay and/or to changes in surface wind forcing, with time scales of several days or less, (4) a major reduction in surface salinity occurred in the immediate vicinity of the mouth of CB between the 14th and 19th of September, based on observations from the salinity mapper which were not reflected in the model results, (5) the effect of salinity forcing on the model-produced surface currents, although noticeable, was less important than the effect of wind forcing, and (6), the strength of the model's halocline tended to weaken proceeding offshore, and that the depth of the halocline decreased from roughly 10 m near the mouth of the Bay to 5 m or so at distances of 60–75 km offshore.

6. DISCUSSION

In this section we discuss several issues directly related to the results which were presented earlier. These topics include the specification of

and Boicourt, 1986). These
e with plume depths inferred
eyond the mouth by Ruzecki
from 5–8 m. On the 20th, the
ate much lower salinities down
on the 14th and may reflect the
discharge that is indicated in
September. However, further
slightly higher salinities within
rofiles. Major differences occur
and the control runs for both
nce of the higher discharge as-
, but these differences decrease
for profiles 7 and 8.
COFS has reproduced essen-
plume, including its preferred
ariability particularly for cases
ponse to southerly winds, (2)
ccur using the daily *versus* the
luding stronger salinity gradi-
(3) the structure of the plume
olume flux at the mouth of the
d forcing, with time scales of
ion in surface salinity occurred
h of CB between the 14th and
tions from the salinity mapper
results, (5) the effect of salinity
e currents, although noticeable,
nd forcing, and (6), the strength
aken proceeding offshore, and
sed from roughly 10 m near the
ances of 60–75 km offshore.

es directly related to the results
pics include the specification of

the initial conditions at the mouth of CB, estimating advective time scales for the Bay, and finally, using the Kelvin number to infer the importance of earth rotation in deflecting the plume.

6.1. Initial Conditions at the Mouth of the Bay

From results presented in the last section, the model-generated salinities in the near-field region of the plume for the 14th and 19th of September were not necessarily consistent with the corresponding maps of surface salinity from the salinity mapper. Near-field salinities from the model hindcasts where the daily discharge function was used differed only slightly for the two dates, whereas the results from the salinity mapper showed that the near-field salinities had actually decreased significantly (~ -5 psu) over the same time period. The plume structures which were generated in the various model runs may depart from reality for a number of reasons.

First, because we used a discharge function which treated the outflows that resulted from HF as a single pulse rather than including lags for each inflow component, the outflow from CB that was specified may not be realistic. In order to construct a realistic discharge function, it would be necessary to run a 3-D circulation model for CB with initial conditions, surface forcing, and boundary conditions appropriate for the period surrounding HF. Such a model could be used to determine the time required for riverine waters entering the Bay at various locations to travel through the bay system until they arrived at the mouth where they would be combined to produce a realistic outflow.

Second, the volume flux was specified for only one grid point due to the lack of spatial resolution near the entrance of the Bay. Thus, the bay outflow is introduced into the model domain as a point source, when in reality, the source should be distributed across the entire mouth. By employing a higher-resolution distributed source across the mouth, we could have prescribed lower salinities at the south end, and higher salinities at the north end, in accordance with the recent observations of Holderied and Valle-Levinson (1997), for example. In the vertical, a simple one-layer approximation that provided a linear decrease in transport with depth was used to distribute the outflow. Based on the observations of Valle-Levinson *et al.* (1997), a two-layer formulation with waters of lower salinity leaving the Bay in the upper

layer and waters of higher salinity entering the Bay in the lower layer would have been much closer to reality.

Third, we assigned a value of 0 psu to the volume flux from CB in our model runs, and even with a value this low, results near the mouth indicate that the model-generated salinities were too high, particularly for the 14th and the 19th of September. Clearly, the assignment of appropriate values for salinity in the near-field is problematic. Finally, although no injection velocity was assigned to the volume fluxes which were specified in our model runs, previous work by Wang and Kravitz (1980) and Chao and Boicourt (1986) indicates it is the potential energy associated with the plume and not the kinetic energy that is most important in influencing the circulation which is induced by the discharge of low salinity water onto the shelf.

Further offshore in the far-field region where realistic atmospheric forcing and other environmental factors could be incorporated, the overall position and orientation of the plume appears to be in reasonable agreement with past observations of this feature (*e.g.*, Munday and Fedosh, 1981; Boicourt *et al.*, 1987). However, on closer inspection, several factors affect the geometry of the model-generated plume which may cause the exact position and orientation of this feature to be unrealistic. First, the origin for the model where the volume flux is specified is the single grid point located at 37.02 N, 76.05 W, a distance of 5 km west-northwest of the actual bay mouth. Although this is a relatively small distance, it alters the path taken by the discharge out of the Bay and onto the shelf, resulting in a small but noticeable difference in the preferred location of the plume at greater distances away from the mouth. Second, the coastal boundary in the model is the 10 m isobath and not the coast itself, a factor which prevents the plume from "hugging" the coast, as it often does, particularly under the influence of winds from the north. According to Chao (1990) on summarizing the results of Boicourt *et al.* (1987), there appear to be two dominant patterns that characterize the CB plume. Under the influence of winds from the north, the seaward extension of the plume is suppressed and it tends to lie next to the coast south of Cape Henry with an intensified coastal jet that follows the coast further down stream. Under the influence of winds from the south, the plume tends to spread seaward with its axis lying further offshore and oriented in a generally southwesterly direction. Based on the ability of COFS to generate plumes for each of the two situations described by Chao, it

appears that the model will produce more realistic plume behavior when surface winds are from the southern sector. This is true because the coastal boundary in the model is located at the 10 m isobath instead of at the coast itself, a constraint which effectively prevents the plume from lying next to the coast.

6.2. Estimating Advective Time Scales for the Bay

Previously, in Section 4, we mentioned the fact that it is difficult to estimate the time required for riverine waters that enter the Bay at various locations to reach the mouth. For barotropic waves, *i.e.*, surface gravity waves, where the water depth, h, is small compared to the wavelength, the phase speed, c, is given by $(gh)^{1/2}$, where g is the acceleration due to gravity. A simple calculation in this case yields time scales on the order of a day or less for shallow-water (*i.e.*, barotropic) waves to propagate through the Bay. This time scale is consistent with our assumption that there are no significant lags associated with riverine waters traveling through the Bay. However, this assumes that the Bay acts as a one-layer system, and, clearly, this is not the case for a significant fraction of CB where a two-layer approximation is in better agreement with observations (*e.g.*, Pritchard, 1952; Wang, 1979). Hess (1986) calculated flow rates for suddenly increased river flows into the Bay and found that increased flows at the mouth occurred with delays of one-to-three tidal cycles, with the increased flow propagating down the Bay at gravity wave speeds. However, during the aftermath of Tropical Storm Agnes (6/72), minimum salinities were not observed at the mouth of the Bay until about a month after peak flooding (Schubel *et al.*, 1976). Holderied and Valle-Levinson (1997) also employ a one-month lag to account for the time required for the effects of river discharge to reach the mouth of the Bay. According to Walstad (personal communication), advective time scales for the internal (*i.e.*, baroclinic) mode range from 10 to 30 days. Such delays would argue against a simple one-layer approximation following major discharge events from the Bay. For a two-layer system, the phase speed for waves where the wavelength is much greater than the water depth can be expressed as

$$c = [g((h_1 h_2/(h_1 + h_2))(\rho_2 - \rho_1/\rho_2))]^{1/2}$$

difference between the plume and the layer below, the Kelvin number will be seasonally dependent and should increase during winter when the density difference is a minimum.

7. SUMMARY AND CONCLUSIONS

The purpose of the work presented here has been to determine the ability of the Coastal Ocean Forecast System, given the existing model constraints, to portray the structure and evolution of the low salinity plume formed by the discharge of low salinity water from CB following a major discharge event. Realistic tidal and wind forcing were included. Monthly climatological outflow data for CB that are used routinely in the model were also included in a parallel model run in order to determine the impact of discharge from the Bay on the behavior of the plume. Observations of surface salinity from a recently-developed airborne microwave radiometer, *i.e.*, salinity mapper, were included for comparison with, and evaluation of, COFS, particularly in the near-field region of the plume. In the absence of observations, a discharge function was constructed to specify the outflow from CB following HF based essentially on a simple summation of the major river inputs. This scenario is consistent with waters which travel through the Bay at barotropic wave speeds, but not consistent with baroclinic wave speeds which indicate circulation time scales on the order of a month. The resulting discharge time history concentrated the primary outflow over a period of just 3 days or so, producing what was expected to be the maximum impact on the behavior of the low salinity plume.

The salinity maps from the salinity mapper revealed a significant reduction in surface salinity near the bay mouth between the 14th and the 19th of September 1996. The model-generated salinity maps, however, did not indicate such a trend. This discrepancy can be attributed to the inherent difficulties in specifying the initial conditions at the mouth of the Bay including a discharge function which was most likely unrealistic, and the relatively coarse spatial resolution of the model. Although the salinity maps from the airborne radiometer extended only 20–25 km offshore and covered primarily the near-field region of the plume, the model results extended almost 100 km

offshore and, thus, covered the far field region of the plume as well. We have no direct verification of the model results beyond ~25 km from the bay mouth, but our expectation is that they should be far more realistic due to the increasing influence from, and/or interaction with, such factors as atmospheric forcing, earth rotation, mixing, interaction with the prevailing circulation, and possible bathymetric influence. The plume structures that were generated in the model in the far field region are consistent with this interpretation, and are in general agreement with past observations of this feature. In this regard, the modeled plume displayed the effect of earth rotation by turning to the right along the coast south of Cape Henry, in general agreement with past observations. This result was further supported by a separate calculation of the Kelvin number which yielded a value that clearly indicated the importance of earth rotation. However, because the coastal boundary for the model corresponds to the 10 m isobath and not to the coast *per se*, the model should produce a plume with the proper location and orientation in cases where it is located away from the coast which often occurs when the prevailing winds are from the south.

A major result from the simulations was that our use of a discharge function based on daily observed river inflows to the Bay showed significant improvements in characterizing the plume as compared to the monthly climatological outflow time history that is presently used in the model. In particular, the salinity gradients in the region of the plume were much stronger for the hindcasts than they were for the control runs. Based on these results, it is recommended that daily observed and forecast outflows be used in the COFS wherever they are available within the model domain in place of the climatological outflows that are presently used.

The surface circulation off the mouth of the Bay was strongly influenced by the local winds and to a lesser, but noticeable, extent by the strong salinity gradients around the periphery of the plume, according to the model results. Also, the structure of the plume changed rapidly in response to rapid changes in outflow from the Bay, to changes in wind forcing, or to both, on time scales of several days or less.

Although the primary emphasis in this study was on the ability of the model to characterize the surface manifestation of the CB plume,

the model was also used to construct a sequence of vertical profiles of salinity along a line close to the axis of the plume. The strength of the halocline tended to weaken offshore. Also, the depth of the halocline decreased from roughly 10 m near the mouth of the Bay to depth of 5 m or so at distances of 60–75 km offshore.

It is a difficult task to construct discharge functions that realistically portray the outflow from CB. This problem arises, first, because direct observations are lacking, and, second, because it is difficult to estimate the time required for riverine waters which enter the Bay at various locations to circulate through the bay system until they reach the mouth. Studies are needed to provide additional guidance in this area.

In the future the possibility of acquiring surface salinities on a regular basis would provide a new source of data which could be assimilated into coastal circulation models such as the COFS. This information would be particularly useful along the U.S. East Coast where a number of major rivers and bays feed directly into coastal waters.

Acknowledgments

Thanks to the following individuals for providing various forms of support and counsel during the period of this study: Frank Aikman, Carl Cerco, Ping Chen, Richard Garvine, Mark Goodberlet, Zhen Li, Scott Philips, D. B. Rao, Arnoldo Valle-Levinson and Leonard Walstad. The NOAA Airborne Scanning Low Frequency Microwave Radiometer was developed under funding from the Small Business Innovative Research Program of the Department of Commerce. It is with deep sorrow that we acknowledge the death of Dr. Jim Zaitzeff. Jim was essentially the inspiration behind the salinity mapper whose development he shepherded from its inception to its present status.

References

Aikman, F., Wei, E. J. and Shultz, J. R. (1998) Water level evaluation for the Coastal Ocean Forecast System. *Preprint: AMS Second Conference on Coastal Atmospheric and Oceanic Prediction and Processes*, 11–16 January 1998, Phoenix, Arizona, 1–6.

Army Corps of Engineers, 1975: *Impact of Tropical Storm Agnes on Chesapeake Bay*, Summary. Baltimore District, Department of the Army, p. 46.

Beardsley, R. C. and Hart, J. (1978) A simple theoretical model for the flow of an estuary onto a continental shelf. *Journal of Geophysical Research*, **83**, 873–883.

truct a sequence of vertical profiles of
axis of the plume. The strength of the
nore. Also, the depth of the halocline
ar the mouth of the Bay to depth of
km offshore.
t discharge functions that realistically
his problem arises, first, because direct
cond, because it is difficult to estimate
aters which enter the Bay at various
the bay system until they reach the
ovide additional guidance in this area.
acquiring surface salinities on a regular
ce of data which could be assimilated
such as the COFS. This information
ig the U.S. East Coast where a number
rectly into coastal waters.

duals for providing various forms of
period of this study: Frank Aikman,
l Garvine, Mark Goodberlet, Zhen Li,
rnoldo Valle-Levinson and Leonard
Scanning Low Frequency Microwave
der funding from the Small Business
of the Department of Commerce. It is
owledge the death of Dr. Jim Zaitzeff.
ion behind the salinity mapper whose
m its inception to its present status.

R. (1998) Water level evaluation for the Coastal
AMS Second Conference on Coastal Atmospheric
es, 11–16 January 1998, Phoenix, Arizona, 1–6.
ct of Tropical Storm Agnes on Chesapeake Bay,
partment of the Army, p. 46.
imple theoretical model for the flow of an estuary
f Geophysical Research, **83**, 873–883.

Black, T. L. (1994) The new NMC mesoscale Eta model: description and forecast examples. *Weather and Forecasting*, **9**, 265–278.

Blumberg, A. F. and Grehl, B. J. (1987) A river flow climatology for the United States Atlantic coast. Hydroqual, Inc., Mahwah, New Jersey, p. 6 [Available from Hydroqual, Inc., 1 Lethbridge Plaza, Mahwah, N.J. 07430].

Blumberg, A. F. and Mellor, G. L. (1987) A description of a three-dimensional coastal ocean circulation model. *Three-Dimensional Coastal Ocean Models*, Vol. 4, Heaps, N., Editor, American Geophysical Union, pp. 1–16.

Blume, H.-J. C., Kendall, B. M. and Fedors, J. C. (1978) Measurement of ocean temperature and salinity via microwave radiometry, *Boundary Layer Meteorology*, **13**, 295–308.

Boicourt, W. C. (1973) The circulation of water on the continental shelf from Chesapeake Bay to Cape Hatteras. *Ph.D. Thesis*, The Johns Hopkins University, Baltimore, Maryland, p. 183.

Boicourt, W. C. (1981) Circulation in the Chesapeake Bay entrance region: estuary-shelf interaction. *Chesapeake Bay Plume Study, Superflux 1980*, Campbell, J. W. and Thomas, J. P., Eds., *NASA Conf. Pub. 2188*, NOAA/NEMP III 81 ABCDFG 0042, pp. 61–78.

Boicourt, W. C., Chao, S.-Y., Ducklow, H. W., Gilbert, P. M., Malone, T. C., Roman, M., Sanford, L. P., Fuhrman, J., Garside, C. and Garvine, R. (1987) Physics and microbial ecology of a buoyant estuarine plume on the continental shelf. *EOS*, **69**, 666–668.

Chao, S.-Y. and Boicourt, W. C. (1986) Onset of estuarine plumes. *J. Phys. Oceanogr.*, **16**, 2137–2149.

Chao, S.-Y. (1988a) River-Forced estuarine plumes. *J. Phys. Oceanogr.*, **18**, 72–88.

Chao, S.-Y. (1988b) Wind-driven motion of estuarine plumes. *J. Phys. Oceanogr.*, **18**, 1144–1166.

Chao, S.-Y. (1990) Tidal modulation of estuarine plumes. *J. Phys. Oceanogr.*, **20**, 1115–1123.

Chen, P. and Mellor, G. L. (1998) Determination of tidal boundary forcing using tide station data. Coastal Ocean Prediction, Mooers, C. N. K., Editor, AGU/CES.series, in press.

Dengg, J., Beckmann, A. and Gerdes, R. (1996). The Gulf stream separation problem. *The Warmwatersphere of the North Atlantic Ocean*, Krauss, W., Editor, Gebrader Borntraeger, Berlin, pp. 253–290.

Garvine, R. W. (1987) Estuary plumes and fronts in shelf waters: a layer model. *J. Phys. Oceanogr.*, **17**, 1877–1896.

Garvine, R. W. (1995) A dynamical system for classifying buoyant coastal discharges. *Continental Shelf Research*, **15**, 1585–1596.

Goodberlet, M., Swift, C., Kiley, K., Miller, J. and Zaitzeff, J. (1997) Microwave remote sensing of coastal zone salinity. *Journal of Coastal Research*, **13**, 363–372.

Goodrich, D. M. (1987) Nontidal exchange processes at the Chesapeake Bay entrance. In: *Hydraulic Engineering 1987*, Ragan, R., Ed., American Society of Civil Engineers, New York, pp. 493–498.

Harrison, W., Brehmer, M. and Stone, R. (1964) Nearshore tidal and nontidal currents, Virginia Beach, Virginia. U.S. Army Coastal Engineering Research Center, Technical. Memorandum No. 5.

Hess, K. W. (1986) Numerical model of circulation in Chesapeake Bay and the continental shelf. *NOAA Technical Memorandum NESDIS AISC 6*, U.S. Dept. Of Commerce, Washington, D.C., 47 p.

Hess, K. W. (1989) MECCA program documentation. NOAA Technical Report NESDIS 24, U.S. Department of Commerce, 258 p.

Holderied, K. and Valle-Levinson, A. (1997) Hydrographic and flow structure in the Chesapeake Bay mouth and plume region under high freshwater discharge conditions. Submitted to *Continental Shelf Research*.

James, I. D. (1997) A numerical model of the development of anticyclonic circulation in a gulf-type region of freshwater influence. *Continental Shelf Research*, **17**, 1803–1816.

Kelley, J. G. W., Thiebaux, H. J., Chalikov, D. and Behringer, D. W. (1997) Impact of data assimilation in the Coastal Ocean Forecast System. *Proceedings of the Second Conference on Coastal Atmospheric and Oceanic Prediction and Processes*, American Meteorological Society, 11–16 January 1998, Phoenix, Arizona, 7–10.

Kendall, B. M. (1981) Remote sensing of the Chesapeake Bay plume, salinity via microwave radiometry. Chesapeake Bay Plume Study, Superflux 1980, Campbell, J. W. and Thomas, J. P., Editors, *NASA Conf. Pub. 2188*, NOAA/NEMP III 81 ABCDFG 0042, pp. 131–140.

Koutitonsky, V. G. and Bugden, G. L. (1991) The physical oceanography of the Gulf of St. Lawrence: a review with emphasis on the synoptic variability of the motion. *The Gulf of St. Lawrence: Small Ocean or Big Estuary*?, Therriault, J.-C., Editor, Canadian Special Publication of Fisheries and Aquatic Science, **113**, 57–90.

Kuo, A. Y., Ruzecki, E. P. and Fang, C. S. (1976) The effects of the Agnes flood on the salinity structure of the lower Chesapeake Bay and contiguous waters. In: *The Effects of Tropical Storm Agnes on the Chesapeake Bay Estuarine System*. Ruzecki, E. P. *et al.*, Editors, The Chesapeake Research Consortium, Inc., CRC Publication No. 54, The Johns Hopkins University Press, Baltimore and London, pp. 81–103.

Mellor, G. L. and Yamada, T. (1982) Development of a turbulent closure model for geophysical fluid problems. *Reviews of Geophysics and Space Physics*, **20**, 851–875.

Miller, J. L., Goodberlet, M. A. and Zaitzeff, J. B. (1998) Airborne salinity mapper makes debut in coastal zone. *EOS*, **79**, 173.

Norcross, J. J. and Stanley, E. M. (1967) Inferred surface and bottom drift. Circulation of Shelf Waters off the Chesapeake Bight, ESSA Professional Paper 3, Harrison, W., Norcross, J. J., Pore, N. A. and Stanley, E. M., Editors, U.S. Dept. of Commerce, Washington, D.C., pp. 11–42.

O'Connor, W. P. (1991) A user's manual for the Princeton Ocean Model. Institute for Naval Oceanography Report SP-5, Stennis Space Center, MS, 69 p.

O'Donnell, J. (1990) The formation and fate of a river plume: a numerical model. *J. Phys. Oceanogr.*, **20**, 551–569.

Oey, L.-Y. and Mellor, G. L. (1993) Subtidal variability of estuarine outflow, plume, and coastal current: a model study. *J. Phys. Oceanogr.*, **23**, 164–171.

Pritchard, D. W. (1952) Salinity distribution and circulation in the Chesapeake Bay estuarine system. *J. Mar. Res.*, **11**, 106–123.

Reyes-Hernandez, C. and Valle-Levinson, A. (1997) Monthly hydrography in the lower Chesapeake Bay, 1996 data report. CCPO Technical Report 97–04, Center for Coastal Physical Oceanography, Old Dominion University, Norfolk, Virginia, 70 p.

Ruzecki, E. P., Welch, C. S., Usry, J. and Wallace, J. W. (1976) The use of the EOLE satel lite system to observe continental shelf circulation. *Eighth Annual Offshore Technology Conference 2*, paper No. 2592, pp. 697–708.

Ruzecki, E. P. (1981) Temporal and spatial variations of the Chesapeake Bay plume. *Chesapeake Bay Plume Study, Superflux 1980*, Campbell, J. W. and Thomas, J. P., Editors, *NASA Conf. Pub. 2188*, NOAA/NEMP III 81 ABCDFG 0042, pp. 111–130.

Schubel, J. R., Carter, H. H. and Cronin, W. B. (1976) Effects of Agnes on the distribution of salinity along the main axis of the bay and in contiguous shelf waters. In: *The Effects of Tropical Storm Agnes on the Chesapeake Bay Estuarine System*, Ruzecki, E. P. *et al.*, Editors, The Chesapeake Research Consortium, Inc., CRC Publication No. 54, The Johns Hopkins University Press, Baltimore and London, pp. 33–65.

Teague, W. J., Carron, M. J. and Hogan, P. J. (1990) A comparison between the generalized digital environmental model and Levitus climatologies. *J. Geophys. Res.*, **95**, 7167–7183.

Thomas, J. P. (1981) Assessment
monitoring. *Chesapeake Bay P*
Thomas, J. P., Editors, *NASA*
0042, pp. 503–515.

U.S. Department of Commerce (199
September 8, 1996. U.S. De
Atmospheric Administration, N

Valle-Levinson, A. and Lwiza, K. M
exchange between the Chesape
100, 18551–18563.

Valle-Levinson, A., Li, C., Royer, T
Chesapeake Bay entrance. Subı

Wang, D. P. (1979) Wind-driven
J. Phys. Oceanogr., **9**, 564–572

Wang, D.-P. and Kravitz, D. W.
estuarine circulation. *J. Phys.*

Weaver, A. J. and Hsieh, W. W. (19
continental shelf circulation. *J.*

Wheless, G. H. and Klinck, J. M. (1
sloping bottom topography. *J.*

Wheless, G. H. and Valle-Levinsc
estuarine exchange through a
101, 25675–25687.

Wiseman, W. J. and Garvine, R. W
mouths. *Estuaries*, **18**, 509–51

Zhang, Q. H., Janowitz, G. S. and
and shelf waters: a model and

Thomas, J. P. (1981) Assessment of Superflux relative to fisheries research and monitoring. *Chesapeake Bay Plume Study, Superflux 1980*, Campbell, J. W. and Thomas, J. P., Editors, *NASA Conf. Pub. 2188*, NOAA/NEMP III 81 ABCDFG 0042, pp. 503–515.

U.S. Department of Commerce (1997) Service Assessment, Hurricane Fran, August 28–September 8, 1996. U.S. Department of Commerce, National Oceanic and Atmospheric Administration, National Weather Service, Silver spring, MD, 27 p.

Valle-Levinson, A. and Lwiza, K. N. M. (1995) The effects of channels and shoals on exchange between the Chesapeake Bay and the adjacent ocean. *J. Geophys. Res.*, **100**, 18551–18563.

Valle-Levinson, A., Li, C., Royer, T. C. and Atkinson, L. P. (1997) Flow patterns at the Chesapeake Bay entrance. Submitted to Continental Shelf Research.

Wang, D. P. (1979) Wind-driven circulation in the Chesapeake Bay, Winter 1975. *J. Phys. Oceanogr.*, **9**, 564–572.

Wang, D.-P. and Kravitz, D. W. (1980) A semi-implicit two-dimensional model of estuarine circulation. *J. Phys. Oceanogr.*, **10**, 441–454.

Weaver, A. J. and Hsieh, W. W. (1987) The influence of buoyancy flux from estuaries on continental shelf circulation. *J. Phys. Oceanogr.*, **17**, 2127–2140.

Wheless, G. H. and Klinck, J. M. (1995) The evolution of density-driven circulation over sloping bottom topography. *J. Phys. Oceanogr.*, **25**, 888–901.

Wheless, G. H. and Valle-Levinson, A. (1996) A modeling study of tidally driven estuarine exchange through a narrow inlet onto a sloping shelf. *J. Geophys. Res.*, **101**, 25675–25687.

Wiseman, W. J. and Garvine, R. W. (1995) Plumes and coastal currents near large river mouths. *Estuaries*, **18**, 509–517.

Zhang, Q. H., Janowitz, G. S. and Pietrafesa, L. J. (1987) The interaction of estuarine and shelf waters: a model and applications. *J. Phys. Oceanogr.*, **17**, 455–469.

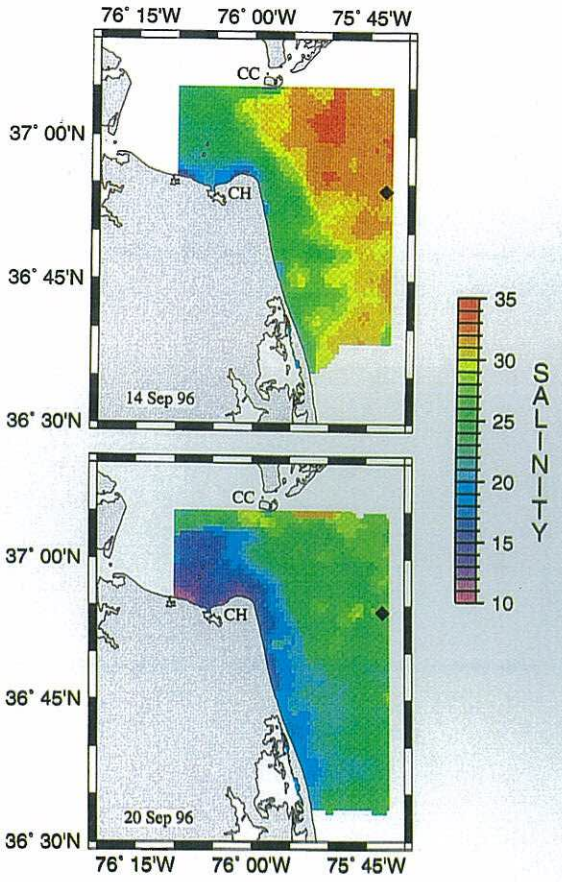

COLOR PLATE II Maps of surface salinity obtained from the Scanning Low-Frequency Microwave Radiometer for September 14 (upper panel) and September 20 (lower panel), 1996. "CC" refers to Cape Charles located at the north end of the entrance to Chesapeake Bay, and "CH" refers to Cape Henry located at the south end of Chesapeake Bay. The distance from Cape Charles to Cape Henry is approximately 15 km. Each pixel represents a one km^2 area. (See L. C. Breaker *et al.* page 325).